Chinese Physics Letters

中国物理学会
Chinese Physical Society

REVIEW

Theoretical Models on Interfacial Thermal Conductance of Nanoscale Solid Interfaces in Chips: A Mini Review

To cite this article: Zhicheng Zong *et al* 2024 *Chinese Phys. Lett.* **41** 106301

View the article online for updates and enhancements.

You may also like

- Complete Universal Scaling in First-Order Phase Transitions
Fan Zhong and
- Magnetism Measurements of Two-Dimensional van der Waals Antiferromagnet $CrPS_4$ Using Dynamic Cantilever Magnetometry
Qi Li, , Weili Zhen et al.
- Normal and Superconducting Properties of $La_3Ni_2O_7$
Meng Wang, , Hai-Hu Wen et al.

This content was downloaded from IP address 115.156.143.154 on 09/10/2024 at 05:19

Chinese Physics Letters **41**, 106301 (2024) **Review**

Theoretical Models on Interfacial Thermal Conductance of Nanoscale Solid Interfaces in Chips: A Mini Review

Zhicheng Zong(宗志成)[1], Xiandong Chen(陈显栋)[2,3*], Bin Yan(严斌)[2,3], Yelei Xie(谢业磊)[2,3], Jian Pang(庞健)[2,3], Guangyao Li(李光耀)[2,3], Jiqiang Hu(胡继强)[1], Zhipeng Wu(吴志鹏)[1], Bo Li(李博)[1], Haisheng Fang(方海生)[1], and Nuo Yang(杨诺)[1*]

[1]*School of Energy and Power Engineering, Huazhong University of Science and Technology, Wuhan 430074, China*
[2]*Department of Packaging and Testing Institution, Sanechips Technology Co., Ltd., Shenzhen 518055, China*
[3]*State Key Laboratory of Mobile Network and Mobile Multimedia Technology, ZTE Corporation, Shenzhen 518055, China*

(Received 1 April 2024; accepted manuscript online 21 September 2024)

With the rapid increase in power density of electronic devices, thermal management has become urgent for the electronics industry. Controlling temperature in the back-end-of-line is crucial for maintaining the reliability of integrated circuits, where many atomic-scale interfaces exist. The theoretical models of interface thermal conductance not only accurately predict the values but also help to analyze the underlying mechanism. This review picks up and introduces some representative theoretical models considering interfacial roughness, elastic and inelastic processes, and electron–phonon couplings, etc. Moreover, the limitations and problems of these models are also discussed.

DOI: 10.1088/0256-307X/41/10/106301

1. Introduction. Interfacial thermal conductance (ITC) is increasingly focused due to its important effects in chips, thermoelectrics, opticelectrics, and solid-state batteries.[1–5] The rapid advancement of nanotechnologies has led to a gradual reduction in sizes of materials to nanoscales. ITC becomes crucial in devices where size reduction is employed to enhance operating frequency or to achieve high local power density.[6,7] This significance is particularly pronounced in nanoscale devices, such as chips, where the thermal resistance between interfaces frequently dictates the overall thermal resistance of the devices.

Understanding the mechanism of ITC is crucial for comprehending the significant impact of ITC on heat dissipation of chips,[6,8] particularly within the back-end-of-line (BEOL) chips. Chip manufacturing is usually composed of two major stages: front end of line (FEOL) and BEOL. In the BEOL, there are commonly numerous interfaces, as illustrated in Fig. 1(a), comprising metal/dielectric and dielectric/dielectric interfaces. The thermal interface resistance serves as the primary heat pathway to the BEOL and is thus crucial to evaluate the significance of interface thermal resistance accurately.[9] When investigating thermal resistance in the BEOL, Chung *et al.*[10] discovered a notable 42 K disparity between scenarios where interface thermal resistance in BEOL was considered and when it was not. This finding underscores the significance of interface thermal resistance in BEOL. Managing thermal conditions in the BEOL is crucial for maintaining the reliability of integrated circuits, as elevated temperatures accelerate the degradation of both BEOL and FEOL components.[11] In addition to reliability concerns, the relentless pursuit of marginal improvements in current within advanced complementary metal oxide semiconductor (CMOS) technologies underscores the importance of understanding interfacial thermal resistances in the BEOL.[9] Figure 1(b) illustrates the thermal transport mechanism at the interfaces in the BEOL, including interfacial roughness, phonon–phonon coupling (both elastic and inelastic processes), and electron–phonon coupling.

In the study of interface thermal conductance, there are theoretical model calculations, numerical simulation, and experimental measurement. In numerical simulation, molecular dynamics (MD)[12,13] and atomistic Green's function (AGF)[14,15] have demonstrated accurate capabilities in simulating ITC. Yang *et al.*[16] simulated the ITC of an Al/Si interface using MD and observed the existence of interfacial phonon modes. Yang *et al.*[15] used the AGF method to investigate the underlying physical mechanism of the effect of mass distribution in one-dimensional atomic chains on ITC. However, the intricacies of MD modeling and the computational complexity of AGF matrix solving hinder quick predictions of interface thermal conductance. Several experimental measurement methods, such as 3-Omega,[17] time-domain thermoreflectance (TDTR),[18,19] and frequency domain thermoreflectance (FDTR),[20] have achieved maturity in quantifying ITC. Other experimental methods, such as scanning transmission electron microscopy (STEM), have also contributed to the research of ITC. In the investigation of cubic boron nitride/diamond heterointerfaces, Qi *et al.*[21] found the presence of interfacial phonon modes by using STEM. Then, Li *et al.*[22]

*Corresponding authors. Email: chen.xiandong@sanechips.com.cn; nuo@hust.edu.cn
© 2024 Chinese Physical Society and IOP Publishing Ltd

also observed interfacial phonon modes in AlN/Al and AlN/Si interfaces by STEM. Despite their maturity, the high cost of measurements and the intricate nature of interface preparation impede swift predictions of interface thermal conductivity. In comparison to previous simulation and experimental approaches, theoretical models offer a faster means to predict interface thermal conductance. Moreover, theoretical models provide additional insights to comprehend the underlying mechanisms governing interface thermal conductivity. Therefore, research of more accurate theoretical models is of great importance.

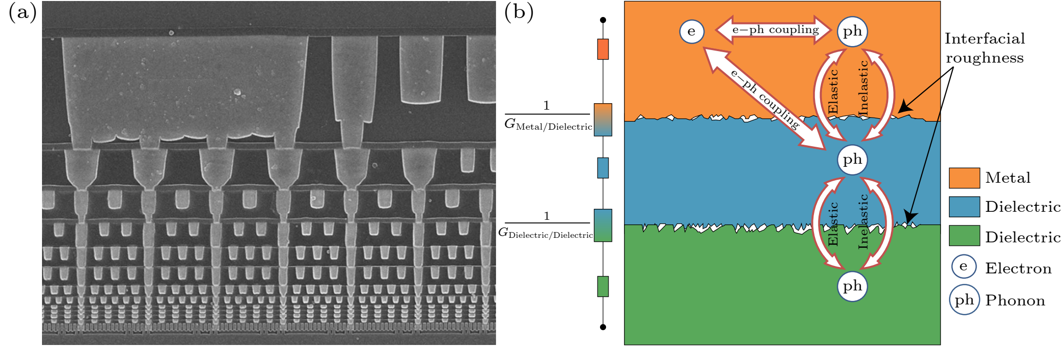

Fig. 1. (a) Schematic representation of interfaces within BEOL. Reproduced with permission.[23] Copyright of IOP Publishing. (b) The bidirectional arrow markers depict the coupling between heat energy carriers (electrons and phonons), resulting in ITC.

In this review, theoretical models to predict ITC are summarized, and future challenges are prospected. Considering the ITC problems in the chip architecture BEOL mentioned above, the corresponding theoretical models to solve the problems are introduced in turn. Firstly, the Landauer formula is introduced for calculating ITC, along with the acoustic mismatch model (AMM) and the diffuse mismatch model (DMM), both of which consider only elastic phonon processes. Secondly, the mixed mismatch model (MMM) is presented, which considers the roughness of the interface. Thirdly, it gives an introduction to theoretical models including inelastic processes on ITC. Fourthly, the contribution of electrons to ITC alongside phonons is acknowledged, prompting the introduction of the electron–electron and electron–phonon coupling mechanism at interfaces. Lastly, theoretical models predicting ITC are summarized, and existing challenges and prospects are presented.

2. Theoretical Model. The Landauer formula is a commonly employed method for predicting ITC. In the interface composed of materials A and B, when heat flows from A to B, there will be resistance at the interface, resulting in a temperature decrease ΔT. The resistance that hinders heat flow is known as the interface thermal resistance, and its reciprocal is the ITC. Considering the interface between the two materials discussed above, an incident phonon on the interface with frequency ω and mode j can either scatter back into material A or propagate into material B. Once the phonon transmission coefficient $\alpha_{\text{A}\to B}(\omega)$ is determined, it enables the calculation of the ITC as[2,24]

$$G=\frac{1}{4}\sum_{j}\int_{0}^{\omega_{\text{cut}}}D_{\text{A},j}(\omega)\frac{\partial f(\omega,T)}{\partial T}v_{\text{A},j}(\omega)\hbar\omega\alpha_{\text{A}\to B,j}(\omega)d\omega. \tag{1}$$

Here, ω_{cut} represents the cut-off frequency, $D_{\text{A},j}(\omega)$ is the phonon density of states, $v_{\text{A},j}(\omega)$ denotes the group velocity, the subscript j corresponds to phonon polarization, and $f(\omega,T)$ is the Bose–Einstein distribution function. However, calculating phonon transmission can be a challenging task, leading to the proposal of various models aimed at simplifying this calculation.

2.1 Elastic Phonon Process. In the AMM, as shown in Fig. 2(a), there is a fundamental assumption that phonons are treated as continuous media, and the interface is considered to be a perfect mirror. This implies that phonons behave as plane waves, and the materials composing the interface are treated as continuous media. This model holds true when the phonon wavelength exceeds the interfacial roughness ($\lambda\gg\eta$), which means that AMM works for extremely smooth interfaces.[2] It is worth noting that directionality needs to be paid attention to when using the AMM model. Incident phonons and transmission phonons must obey Snell's law. When the velocity of the phonon group of material A is greater than that of material B, the phonons from material A can be transmitted through the interface at any incidence angle. In the opposite direction, the incidence angle of material B cannot exceed the critical angle to avoid the occurrence of total reflection. Then the phonon transmission coefficient can be calculated by[2]

$$\alpha_{\text{AMM},\text{A}\to\text{B}}=\frac{4\rho_{\text{A}}v_{\text{A}}\rho_{\text{B}}v_{\text{B}}}{(\rho_{\text{A}}v_{\text{A}}+\rho_{\text{B}}v_{\text{B}})^2}, \tag{2}$$

where ρ_{A} and ρ_{B} denote the mass densities of materials A and B, v_{A} and v_{B} represent the velocities of the phonon groups of materials A and B, respectively.

Contrary to the AMM assumption that phonons do not scatter at the interface, the DMM model posits the opposite, suggesting that all phonons diffuse at the interface, as shown in Fig. 2(b). In this scenario, phonon transmission is governed by the mismatch in the density of phonon states between both sides of the interface. The presence of diffuse scattering disrupts the acoustic correlation between the incident and outgoing phonons, rendering the assumption in DMM that the scattered phonon forgets all incident in-

formation. Consequently, the probability of the scattered phonon traversing the interface becomes entirely independent of the incident information. The DMM model is better suited for extremely rough interfaces, where the roughness scale and the phonon wavelength satisfy $\lambda \ll \eta$.[24] Alternatively, the DMM cannot fully account for the contribution of long-wave phonons to ITC. The calculation for the phonon transmission coefficient within the context of the DMM model cab be carried out with[2]

$$\alpha_{\rm DMM,A\to B} = \frac{\sum_j D_{{\rm B},j} v_{{\rm B},j}}{\sum_j D_{{\rm A},j} v_{{\rm A},j} + \sum_j D_{{\rm B},j} v_{{\rm B},j}}. \quad (3)$$

Here, D represents the phonon density of states, and v denotes the phonon group velocity for the specific phonon mode with the subscript j referring to the phonon polarization.

As mentioned above, the applicability of AMM/DMM depends on the ratio of phonon wavelength to interfacial roughness. Generally, AMM is more suitable for describing long-wave phonon transmission, while DMM is more suitable for short-wave phonon transmission. In other words, AMM is more effective for smooth interfaces, whereas DMM is better suited for interfaces with larger roughness.

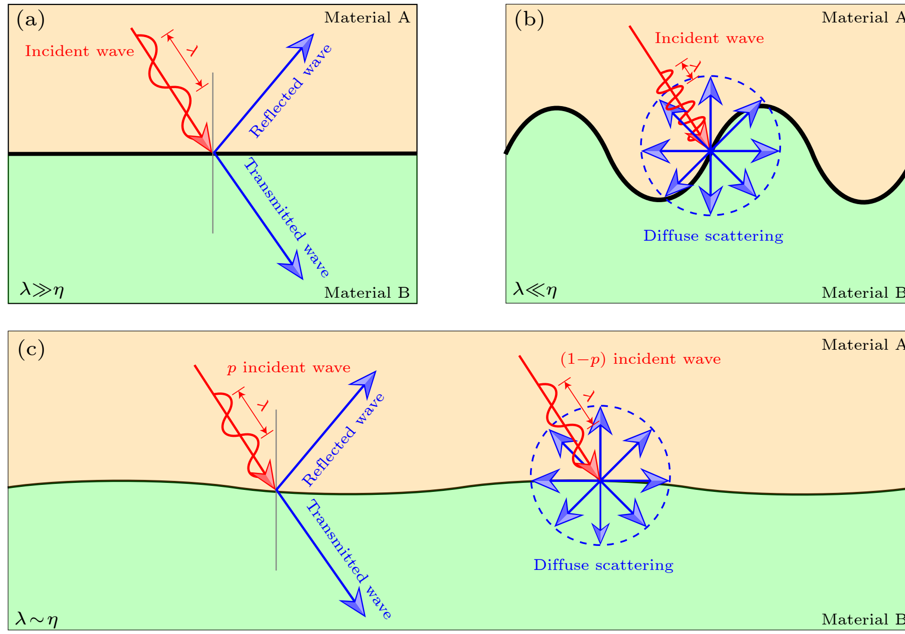

Fig. 2. In AMM (a), phonons undergo specular reflection or refraction, while in DMM (b), phonons experience diffuse scattering. Additionally, in MMM (c), the ratio p of phonons undergoes specular refraction and reflection, while the ratio $(1-p)$ of phonons undergoes diffuse scattering. The scale factor p is contingent upon the phonon wavelength and interfacial roughness.

Zhang *et al.* used AMM and DMM to calculate the phonon transmission coefficient across the Al/Si interface and compared their results with the experimental measurements of Hua *et al.*[25] As shown in Fig. 3(a), the results indicate that at low frequencies (long wavelengths), the phonon transmission coefficient aligns more closely with AMM predictions, while at high frequencies (short wavelengths), it aligns more closely with DMM predictions. Koh *et al.*[26] observed that the interfacial roughness may depend on the thickness of the GaN layers, resulting in different ITC values, as shown in Fig. 3(b). For smoother interfaces (thickness < 40 nm) where phonons exhibit more specular reflection and refraction, the results of ITC align with AMM predictions. For the rougher interfaces (thickness < 40 nm), where phonons exhibit more diffusion, the results of ITC align with DMM predictions. However, AMM or DMM can only provide prediction of ITC for an extreme interfacial structure and cannot consider the practical interfacial structures.[27]

2.2 Roughness. MMM offers a more accurate approach for predicting ITC. At temperatures of 300 K or higher, most phonons have wavelengths comparable to the roughness ($\lambda \sim \eta$),[5] a situation that does not align with the assumptions of the AMM and DMM models. In contrast to the assumptions of AMM and DMM, which both make extreme assumptions about the interface, the MMM takes into account the impact of specific interfacial roughness and contact area on ITC, as shown in Fig. 2(c). In the MMM model, the AMM and DMM models are mixed through the introduction of a specular parameter, denoted as p, as shown by Eq. (4). This parameter signifies that phonons possessing a scale factor of p experience specular reflection at the interface, while the rest of phonons undergo diffuse scattering. The value of the specular parameter p is intricately linked to both interfacial roughness η and the wavelength of phonons λ,

$$\alpha_{\rm MMM,A\to B} = p \times \alpha_{\rm AMM,A\to B} + (1-p) \times \alpha_{\rm DMM,A\to B}. \quad (4)$$

Ziman *et al.*[28] noted that the specular parameter p is associated with both the root-mean-square roughness η and the phonon wavelength λ. They established a specific relationship to quantify this association, which is defined as

$$p = \exp\Big(-\frac{16\pi^2\eta^2}{\lambda^2}\Big). \tag{5}$$

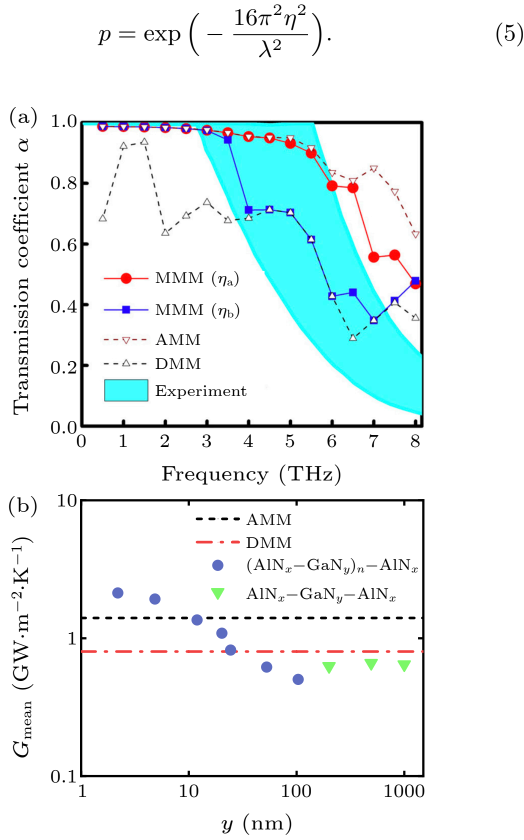

Fig. 3. (a) Comparison of the transmission coefficient α of the AMM, DMM, and MMM (η_a and η_b represent different roughness), with experimental data. Reproduced with permission.[24] Copyright 2018 Zhang, Ma, Zang, Wang and Yang. (b) The mean ITC G_{mean} in the superlattices structures of $(AlN_x\text{-}GaN_y)_n\text{-}AlN_x$ and tri-layers structures of $AlN_x\text{-}GaN_y\text{-}AlN_x$ derived from TDTR measurements compared with AMM and DMM predictions, where $x \approx 4$ nm and y are the thicknesses, $5 < n < 30$ represents the number of periods.[26]

The accuracy of the MMM model is confirmed through the comparison of results obtained from experimental measurements and MD simulations. This model was initially developed by Zhang *et al.*[24] When simulating the Al/Si interface using MD, they extracted roughness data for the interface and incorporated it into the MMM for comparison. As shown in Fig. 3(a), the phonon transmission coefficient predicted by the MMM model is closer to the experimental measurements, where η_a and η_b represent different roughness values. Additionally, comparing MMM predictions of ITC with their own MD simulations reveals that the MMM model considering roughness is more consistent with the MD simulation results, as shown in Fig. 4(a). This comparative analysis of both experimental and simulation results is used to validate the accuracy of the MMM model. Furthermore, it is possible to consider the impact of the interfacial phonon modes on ITC.

However, acquiring interfacial phonon information through MD simulations can be a complex process. Addressing this challenge, Zong *et al.*[29] simplified the application of the MMM by incorporating experimentally measured roughness values and accounting for the impact of the interface structure on the contact area. As shown in Fig. 4(b), the ITC results from the MMM predictions are compared with the experimental measurements from Hopkins *et al.*[30] This simplification enables a straightforward, rapid, and precise prediction of ITC.

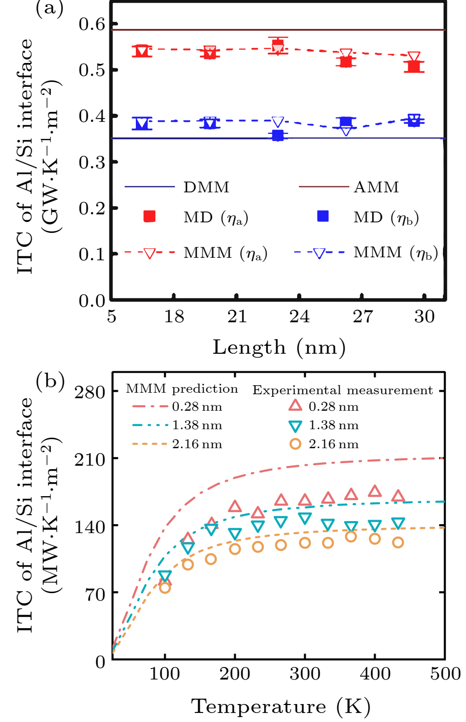

Fig. 4. (a) ITC of the Al/Si interface calculated by the AMM, DMM, and MMM is compared with MD simulations, where η_a and η_b represent different roughness. Reproduced with permission.[24] Copyright 2018 Zhang, Ma, Zang, Wang and Yang. (b) ITC of Al/Si interface calculated MMM is compared with experiments.[29,30] Both the MD simulation results and experiments validate the accuracy of the MMM model.

2.3 Inelastic Phonon Process. Because inelastic phonon process is also important for ITC, it will be introduced that the theoretical modes that consider inelastic phonon processes. The difference between the elastic phonon process and the inelastic phonon process lies in whether the energy of phonons changes across the interface, as shown in Fig. 5. If an inelastic phonon process happens, then the energy can transfer from two or more low-frequency phonons at one side of the interface to one high-frequency phonon at the other side, and vice versa.[31]

Inelastic scattering is an important factor that should be considered in theory, especially at high temperatures or highly mismatched materials.[32–34] Using MD simulation, Landry *et al.*[35] observed that the ITC of Si/Ge interface increases with temperature above 500 K, indicating the growing significance of inelastic processes. In the investigation of Al/Si and Al/GaN interfaces, Li *et al.*[34] similarly noted that inelastic phonon transport processes become prominent at high temperatures. Liu *et al.*[36] introduced Sn particles at the Si/Ge interface to enhance inelastic phonon scattering, thereby improving ITC.

In this section, three models that consider the inelas-

tic phonon process are introduced: the maximum transmission model (MTM),[37] the higher harmonic inelastic model (HHIM),[38] and the anharmonic inelastic model (AIM).[39] Some other models, such as the joint frequency diffuse mismatch model (JFDMM)[40] and scattering-mediated acoustic mismatch model (SMAMM),[41] are available to interested readers for their reference.

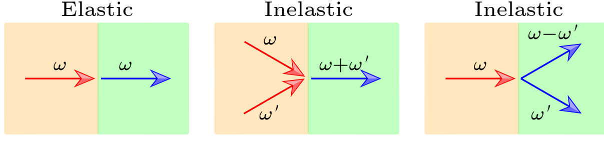

Fig. 5. Elastic phonon process across the interface refers to situations where the phonon energy remains unchanged. Conversely, inelastic phonon process across the interface describes scenarios where the phonon energy undergoes a change.

MTM proposed by Dames and Chen[37] can be considered as an upper limit to ITC accounting for inelastic processes. It treats the transmitted energy of phonons as continuous radiation energy and employs thermal radiation theory under macroscopic conditions for analysis. MTM assumes that phonons of all frequencies in both materials A and B participate in ITC.[39]

In contrary, HHIM proposed by Hopkins[38] can be considered a lower limit to ITC accounting for inelastic processes. For elastic phonon process, HHIM is built on the basis of DMM. For inelastic phonon processes, the HHIM model considers particular multiple phonon interactions occurring at the interface, which restricts its consideration to the whole higher harmonics exclusively. HHIM only accounts for the inelastic processes of n phonons of the same frequency ω to emit a phonon with frequency $n\omega$, such as $\omega_1 + \omega_1 = 2\omega_1$. However, inelastic processes involving n phonons of different frequencies, such as $\omega_1 + \omega_2 = \omega_3$, are not considered. Since HHIM does not account for all possible inelastic processes, it represents a lower limit to ITC.

As shown in Fig. 6, Hopkins *et al.*[39] used DMM, HHIM, and MTM to calculate the ITC of the Pb/diamond interface. In the comparison between the predicted value and the experimental value, DMM could not predict the trend of ITC change with temperature, and seriously underestimated the size of ITC. Incorporating inelastic scattering, HHIM forecasts an ITC surpassing that of the DMM model. While it effectively captures the trend of ITC with temperature, its predicted value remains a lower limit. MTM greatly overestimates the value of ITC, and its predicted temperature dependence trends do not agree well enough with experimentally measured temperature dependence trends. Therefore, a model that compensates for both MTM and HHIM and accurately predicts ITC and temperature dependence is extremely important.

Subsequently, Hopkins *et al.*[39] revisited the consideration of comprehensive inelastic phonon processes and introduced AIM. Similar to HHIM, AIM is built upon the basis of DMM for elastic phonon processes. However, when considering inelastic phonon processes, AIM allows for phonon processes within a specific frequency range, rather than limiting these processes to the whole harmonic frequencies. Then AIM was used to predict the ITC of Pb/diamond interface, as shown in Fig. 6. In the comparison between the predicted value and the experimental value,[42] AIM can not only predict the trend of ITC change with temperature, but also its predicted value is closer to the experimental value.

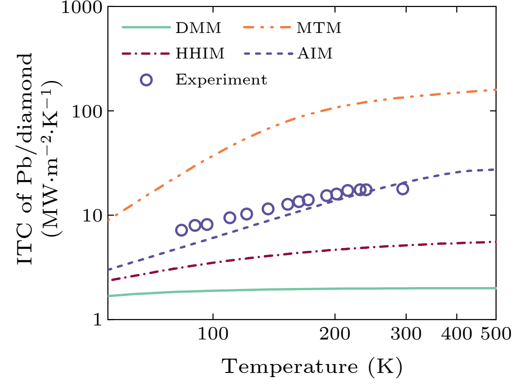

Fig. 6. ITC of the Pb/diamond interface is calculated by DMM, MTM, HHIM and AIM models compared with experimental data.[39,42] Among these models, AIM not only accurately predicts the trend of ITC changes with temperature but also provides values closer to the experimental results.

2.4 Electron–Electron and Electron–Phonon Coupling. In addition to the theoretical models mentioned above, electron contributions to ITC are also significant in metal/metal and metal/dielectric interfaces. Electrons are the primary heat carriers in both metal and metal/metal interfaces. Generally, for the metal/dielectric interface, the contribution of electrons to the ITC can often be ignored above 200 K.[43] However, the contribution of electrons becomes significant, particularly under high non-equilibrium conditions between electrons and phonons[44] or in scenarios with strong electron–phonon couplings, as observed in the investigation of the $TiSi_2$/Si interface.[45] Therefore, it is important to study the physical mechanism and theoretical model of electron influence on ITC of metal/metal interface and metal/dielectric interface.

Since electrons dominate the ITC at metal/metal interfaces, this review focuses exclusively on electronic coupling at these interfaces. The calculation of electronic ITC at metal/metal interfaces can be performed using the Landauer formula[1,5]

$$G = \frac{1}{4}\int_0^{\infty} (\varepsilon - \varepsilon_{\rm F,\,A}) D_{\rm A}(\varepsilon) \frac{\partial f_{\rm A}(\varepsilon)}{\partial T} v_{\rm e,A} \alpha_{\rm e,A\to B}(\varepsilon) d\varepsilon, \quad (6)$$

where ε represents the electron energy, $\varepsilon_{\rm F,\,i}$ denotes the Fermi energy, $D_i(\varepsilon)$ represents the density of electron states, $f_i(\varepsilon)$ is the Fermi distribution function, $v_{\rm e,\,i}$ signifies the electron velocity, i represents metallic material A or B, and $\alpha_{\rm e,\,A\to B}$ denotes the energy-dependent electron transmission coefficient.

Gundrum *et al.*[46] proposed a DMM model for interfacial electron transport across metal/metal interfaces. In this case, the electron transmission coefficient can be cal-

culated by[47]

$$\alpha_{\mathrm{e,A\to B}}(\varepsilon) = \frac{D_{\mathrm{B}}(\varepsilon)[1-f_{\mathrm{B}}(\varepsilon)]v_{\mathrm{B}}(\varepsilon)}{D_{\mathrm{A}}(\varepsilon)f_{\mathrm{A}}(\varepsilon)v_{\mathrm{A}}(\varepsilon)+D_{\mathrm{B}}(\varepsilon)[1-f_{\mathrm{B}}(\varepsilon)]v_{\mathrm{B}}(\varepsilon)}. \tag{7}$$

Exploring the coupling between different energy carriers, such as electrons and phonons, is essential for understanding the contribution of electrons to the ITC of metal/dielectric interfaces. One method of investigating this coupling is the two-temperature model (TTM),[48,49] wherein two types of energy carriers are treated as separate subsystems with coupling interactions, including electron–phonon coupling,[50] magnon-phonon coupling,[51] and phonon–phonon coupling,[52,53] etc.

By using TTM, Wang *et al.* demonstrated that the ITC of metal-dielectric interfaces can be significantly enhanced by carefully selecting materials with strong electron–phonon coupling. Liao *et al.*[51] extended the TTM to incorporate coupled phonon–magnon diffusion.

Additionally, Deng *et al.*[52] provided a review of the application of TTM in phonon–phonon weak coupling. It is classified into two situations: the "implicit coupling" describes couplings within a single structure, such as coupling between different phonon groups, and the "explicit coupling" describes couplings between two structures, such as interfacial thermal conductance.

The electron–phonon coupling in the metal/dielectric interface serves as a prime example for illustrating the application of TTM. For a more detailed derivation of the TTM, interested readers can refer to Refs. [1,47].

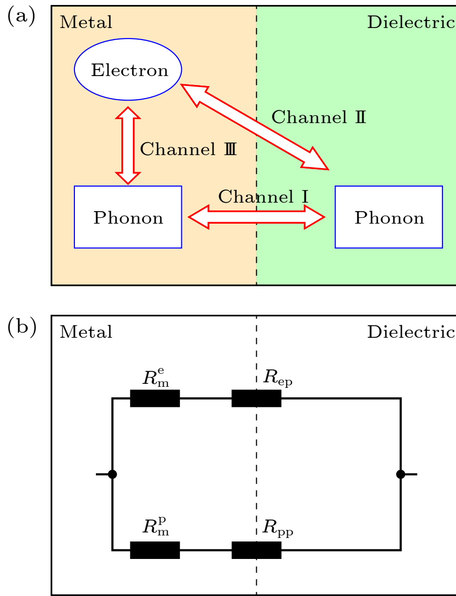

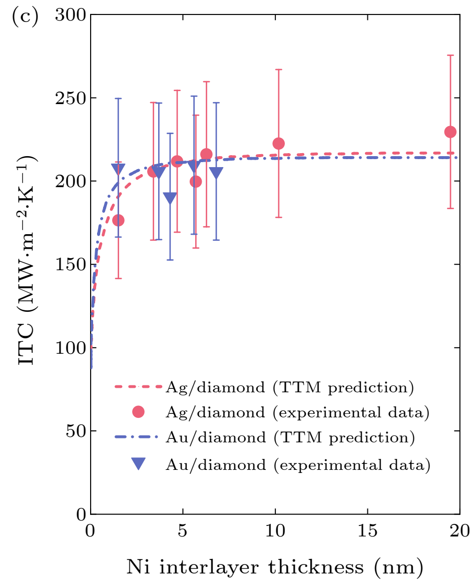

Fig. 7. (a) Description of the three channels of heat transport at the metal/dielectric interface. (b) Illustration of the interface thermal resistance using an equivalent series-parallel thermal resistor network. (c) Influence of a thin Ni interlayer on the ITC at the Ag/Diamond and Au/Diamond interfaces. The TTM predictions are consistent with the experimental data.[54]

The coupling of phonons and electrons at the metal/dielectric interface contributes to ITC through three primary channels, as shown in Fig. 7(a). The phonon–phonon coupling across the metal/dielectric interface serves as the main channel (channel I). Electrons contribute to ITC through two channels. Firstly, electrons can directly couple with phonons in the dielectric across the interface (channel Ⅱ). Secondly, electrons can couple with phonons in metals and then transport across the interface (channel Ⅲ).

Majumdar and Reddy[49] proposed the TTM to explain electron–phonon coupling in metals. Li *et al.*[55] extended TTM further and represented ITC as a series-parallel thermal resistor network incorporating the three channels mentioned above, as shown in Figs. 7(a) and 7(b). They derived a more general form of the ITC:

$$G = \frac{1}{R_{\mathrm{m}}^{\mathrm{e}}+R_{\mathrm{ep}}} + \frac{1}{R_{\mathrm{m}}^{\mathrm{p}}+R_{\mathrm{pp}}}, \tag{8}$$

where the renormalized electronic and lattice thermal resistances are represented by $R_{\mathrm{m}}^{\mathrm{e}} = l/\kappa_{\mathrm{m}}^{\mathrm{e}}$ and $R_{\mathrm{m}}^{\mathrm{p}} = l/\kappa_{\mathrm{m}}^{\mathrm{p}}$, respectively. The width of interfacial area is defined as $l = [(G_{\mathrm{ep}}/\kappa_{\mathrm{m}}^{\mathrm{e}}) + (G_{\mathrm{ep}}/\kappa_{\mathrm{m}}^{\mathrm{p}})]^{-1/2}$ with G_{ep} being the electron–phonon coupling parameter. The phonon–phonon coupling across the metal/dielectric interface R_{pp} can be calculated using the phonon ITC models mentioned above.

However, obtaining the direct coupling between electrons in the metal and phonons in the dielectric across the interface R_{ep} is relatively challenging. Huberman *et al.*,[56] Sergeev,[57] and Mahan[58] have each proposed different theoretical models for the interface, considering electron–phonon coupling to calculate ITC. Interested readers can refer to the relevant literature for further details.[56–58]

Some experimental work verifies the accuracy of the TTM.[54,59,60] Wang *et al.*[60] measured and analyzed the electron–phonon coupling parameter in Au and Cu, finding that the TTM provides accurate predictions.

As illustrated in Fig. 7(c), Blank *et al.*[54] investigated Ag/diamond and Au/diamond interfaces with a Ni interlayer. They employed both TDTR measurements and TTM to determine ITC. The results reveal that ITC increases with the Ni interlayer thickness until reaching a convergent value. The measured values of ITC closely align with the predictions of TTM.

3. Summaries and Outlook. It is of significance to put forward a suitable theoretical model to predict the ITC, not only for the understanding of the thermal transport mechanism but engineering applications. This review primarily delves into the ITC in the BEOL of chips, and focuses on four key mechanisms affecting ITC: elastic phonon processes, inelastic phonon processes, interfacial roughness, and electron–phonon couplings.

The Landauer formula is widely utilized in calculating ITC. The key factor of the formula lies in predicting the phonon transmission coefficient. Different models are proposed to calculate the transmission coefficient and to understand the phonon transport mechanism across interfaces. The classical AMM (DMM) assumes an extremely smooth (rough) interface and treats all phonons as plane waves (diffuse scatterings) at the interface. That is, they do not properly consider the practical interfacial structures.

To address this limitation, the MMM was proposed to account for the effects of arbitrary roughness on ITC. MMM posits that phonons undergo partial specular projection and partial diffuse scattering across the interface, with this ratio determined by the relative relationship between the interfacial roughness and the phonon wavelength. The accuracy of MMM has been validated through both simulations and measurements.

For high temperatures and highly mismatched materials, the inelastic process at the interface is crucial. MTM, HHIM and AIM were proposed to consider inelastic process. MTM assumes that all phonons undergo inelastic processes, which makes it possible to predict the maximum ITC. Conversely, HHIM only considers specific multiple phonon interactions occurring at the interface. AIM aims to incorporate possible phonon inelastic processes as comprehensively as possible to enhance the accuracy of ITC predictions.

Lastly, the contribution of electrons to ITC at metal/metal and metal/dielectric interfaces is reviewed. For metal/metal interfaces, electrons are the main contributors to the ITC, thus only electron–electron couplings are considered and can be described by DMM. For metal/dielectric interfaces, the electron–phonon coupling becomes significant, and its contribution can be divided into three distinct channels. The TTM is introduced to consider the contributions of these three channels to calculate the ITC.

There are still some insufficiencies for the current theoretical models of ITC. They do not encompass the influence of phonon wave-like and coherent behavior. Recent research has indicated that the wave-like and coherent behavior is significant in the ITC of superlattices.[61] As reviewed here, most theoretical models of ITC are based on the Landauer formula, which treats phonon transport as particles across interfaces.

Moreover, the studies by MD simulations have shown that the interface thermal resistance is proportional to the length of the system.[62,63] However, few models incorporate the size effect on phonon transport across interfaces and ITC.

Interfacial phonon modes have emerged as crucial factors in ITC, as observed not only in simulations,[17] but also in experiments.[21,22] However, most theoretical models fail to consider their effect or contribution to ITC.[3] With the support of MD simulations, MMM offers a framework for considering interfacial phonon modes.[24] Understanding interfacial phonon modes is invaluable for comprehending the mechanisms and modulating ITC.

There is a deficiency in understanding the mechanism of ITC of amorphous interfaces, as well as a lack of widely applicable theoretical models for accurately predicting ITC of amorphous interfaces. The results indicate that amorphous interfaces may take higher ITC,[64] yet the underlying mechanism remains elusive. On the basis of DMM, Beechem *et al.*[65,66] proposed a theoretical model considering amorphous interfaces. Unfortunately, these models fail to consider the impact of inelastic phonon processes, thereby restricting their utility to situations where two materials besides interfaces possess similar phonon spectra. Therefore, it is necessary to further study ITC models for predicting amorphous interfaces.

Acknowledgements. This work was supported by the Department of Packaging and Testing Institution of Sanechips. The work was carried out at the National Supercomputer Center in Tianjin, and the calculations were performed on TianHe-HPC.

References

[1] Chen J, Xu X F, Zhou J, and Li B W 2022 *Rev. Mod. Phys.* **94** 025002
[2] Swartz E T and Pohl R O 1989 *Rev. Mod. Phys.* **61** 605
[3] Giri A and Hopkins P E 2020 *Adv. Funct. Mater.* **30** 1903857
[4] Cahill D G, Braun P V, Chen G, Clarke D R, Fan S, Goodson K E, Keblinski P, King W P, Mahan G D, Majumdar A, Maris H J, Phillpot S R, Pop E, and Shi L 2014 *Appl. Phys. Rev.* **1** 011305
[5] Monachon C, Weber L, and Dames C 2016 *Annu. Rev. Mater. Res.* **46** 433
[6] Luo T L, Ding Y F, Wei B J, Du J Y, Shen X Y, Zhu G M, and Li B W 2023 *Acta Phys. Sin.* **72** 234401 (in Chinese)
[7] Wu M, Shi R, Qi R, Li Y, Feng T, Liu B, Yan J, Li X, Liu Z, Wang T, Wei T, Liu Z, Du J, Chen J, and Gao P 2023 *Chin. Phys. Lett.* **40** 036801
[8] Li M, Shakoori M A, Wang R, and Li H 2024 *Chin. Phys. Lett.* **41** 016302
[9] Restrepo O D, Singh D, Rabie M, Paliwoda P, and Silva E C 2022 *IEEE Trans. Electron Devices* **69** 2579
[10] Chung C C, Lin H H, Wan W K, Yang M T, and Liu C W 2019 *IEEE Trans. Electron Devices* **66** 2710
[11] Chang X, Oprins H, Lofrano M, Vermeersch B, Ciofi I, Pedreira O V, Tokei Z, and De Wolf I 2022 *21st IEEE Intersociety Conference on Thermal and Thermomechanical Phenomena in Electronic Systems (iTherm)* 31 May 2022–3 June 2022, San Diego, CA, USA, pp 1–8

[12] Zong Z, Deng S, Qin Y, Wan X, Zhan J, Ma D, and Yang N 2023 *Nanoscale* **15** 16472
[13] Hu S, Zhao C Y, and Gu X 2022 *Chin. Phys. B* **31** 056301
[14] Yang L, Yang B, and Li B 2023 *Phys. Rev. B* **108** 165303
[15] Yang L, Wan X, Ma D, Jiang Y, and Yang N 2021 *Phys. Rev. B* **103** 155305
[16] Yang N, Luo T, Esfarjani K, Henry A, Tian Z, Shiomi J, Chalopin Y, Li B, and Chen G 2015 *J. Comput. Theor. Nanosci.* **12** 168
[17] Deng S, Xiao C, Yuan J, Ma D, Li J, Yang N, and He H 2019 *Appl. Phys. Lett.* **115** 101603
[18] Wilson R B, Apgar B A, Hsieh W P, Martin L W, and Cahill D G 2015 *Phys. Rev. B* **91** 115414
[19] Zheng K, Zhu J, Ma Y M, Tang D W, and Wang F S 2014 *Chin. Phys. B* **23** 107307
[20] Braun J L, Rost C M, Lim M, Giri A, Olson D H, Kotsonis G N, Stan G, Brenner D W, Maria J P, and Hopkins P E 2018 *Adv. Mater.* **30** 1805004
[21] Qi R, Shi R, Li Y, Sun Y, Wu M, Li N, Du J, Liu K, Chen C, Chen J, Wang F, Yu D, Wang E G, and Gao P 2021 *Nature* **599** 399
[22] Li Y H, Qi R S, Shi R C, Hu J N, Liu Z T, Sun Y W, Li M Q, Li N, Song C L, Wang L, Hao Z B, Luo Y, Xue Q K, Ma X C, and Gao P 2022 *Proc. Natl. Acad. Sci. USA* **119** e2117027119
[23] Bernasconi R and Magagnin L 2019 *J. Electrochem. Soc.* **166** D3219
[24] Zhang Y, Ma D, Zang Y, Wang X, and Yang N 2018 *Front. Energy Res.* **6** 48
[25] Koh Y K, Cao Y, Cahill D G, and Jena D 2009 *Adv. Funct. Mater.* **19** 610
[26] Hua C, Chen X, Ravichandran N K, and Minnich A J 2017 *Phys. Rev. B* **95** 205423
[27] Cheng Z 2021 *Acta Phys. Sin.* **70** 236502 (in Chinese)
[28] Ziman J M 1960 *Electrons and Phonons: The Theory of Transport Phenomena in Solids* (Oxford: Oxford University Press)
[29] Zong Z C, Pan D K, Deng S C, Wan X, Yang L N, Ma D K, and Yang N 2023 *Acta Phys. Sin.* **72** 034401 (in Chinese)
[30] Hopkins P E, Duda J C, Petz C W, and Floro J A 2011 *Phys. Rev. B* **84** 035438
[31] Zhou H and Zhang G 2018 *Chin. Phys. B* **27** 034401
[32] Sääskilahti K, Oksanen J, Tulkki J, and Volz S 2014 *Phys. Rev. B* **90** 134312
[33] Feng T, Zhong Y, Shi J, and Ruan X 2019 *Phys. Rev. B* **99** 045301
[34] Li Q, Liu F, Hu S, Song H, Yang S, Jiang H, Wang T, Koh Y K, Zhao C, Kang F, Wu J, Gu X, Sun B, and Wang X 2022 *Nat. Commun.* **13** 4901
[35] Landry E S and McGaughey A J H 2009 *Phys. Rev. B* **80** 165304
[36] Liu Y G, Li H X, Qiu Y J, Li X, and Huang C P 2023 *Phys. Chem. Chem. Phys.* **25** 29080
[37] Dames C and Chen G 2004 *J. Appl. Phys.* **95** 682
[38] Hopkins P E 2009 *J. Appl. Phys.* **106** 013528
[39] Hopkins P E, Duda J C and Norris P M 2011 *J. Heat Transfer* **133** 062401
[40] Hopkins P E and Norris P M 2007 *Nanoscale Microscale Thermophys. Eng.* **11** 247
[41] Prasher R S and Phelan P E 2001 *J. Heat Transfer* **123** 105
[42] Lyeo H K and Cahill D G 2006 *Phys. Rev. B* **73** 144301
[43] Singh P, Seong M, and Sinha S 2013 *Appl. Phys. Lett.* **102** 181906
[44] Giri A, Gaskins J T, Donovan B F, Szwejkowski C, Warzoha R J, Rodriguez M A, Ihlefeld J, and Hopkins P E 2015 *J. Appl. Phys.* **117** 105105
[45] Sadasivam S, Waghmare U V, and Fisher T S 2015 *J. Appl. Phys.* **117** 134502
[46] Gundrum B C, Cahill D G, and Averback R S 2005 *Phys. Rev. B* **72** 245426
[47] Hopkins P E, Beechem T E, Duda J C, Smoyer J L, and Norris P M 2010 *Appl. Phys. Lett.* **96** 011907
[48] Sanders D J and Walton D 1977 *Phys. Rev. B* **15** 1489
[49] Majumdar A and Reddy P 2004 *Appl. Phys. Lett.* **84** 4768
[50] Wang Y, Lu Z, Roy A K, and Ruan X 2016 *J. Appl. Phys.* **119** 065103
[51] Liao B, Zhou J, and Chen G 2014 *Phys. Rev. Lett.* **113** 025902
[52] Deng C, Huang Y, An M, and Yang N 2021 *Mater. Today Phys.* **16** 100305
[53] Wan X, Pan D, Zong Z, Qin Y, Lü J T, Volz S, Zhang L, and Yang N 2024 *Nano Lett.* **24** 6889
[54] Blank M, Schneider G, Ordonez-Miranda J, and Weber L 2019 *J. Appl. Phys.* **126** 165302
[55] Li M, Wang Y, Zhou J, Ren J, and Li B 2015 *Eur. Phys. J. B* **88** 149
[56] Huberman M L and Overhauser A W 1994 *Phys. Rev. B* **50** 2865
[57] Sergeev A V 1998 *Phys. Rev. B* **58** R10199
[58] Mahan G D 2009 *Phys. Rev. B* **79** 075408
[59] Giri A, Gaskins J T, Foley B M, Cheaito R, and Hopkins P E 2015 *J. Appl. Phys.* **117** 044305
[60] Wang W and Cahill D G 2012 *Phys. Rev. Lett.* **109** 175503
[61] Wu X and Han Q 2022 *Int. J. Heat Mass Transfer* **184** 122390
[62] Jones R E, Duda J C, Zhou X W, Kimmer C J, and Hopkins P E 2013 *Appl. Phys. Lett.* **102** 183119
[63] Liang Z, Sasikumar K, and Keblinski P 2014 *Phys. Rev. Lett.* **113** 065901
[64] Zhou W X, Cheng Y, Chen K Q, Xie G, Wang T, and Zhang G 2020 *Adv. Funct. Mater.* **30** 1903829
[65] Beechem T, Graham S, Hopkins P, and Norris P 2007 *Appl. Phys. Lett.* **90** 054104
[66] Beechem T and Hopkins P E 2009 *J. Appl. Phys.* **106** 124301